Impaired Proliferation, Apoptosis, and Angiogenesis of Adipose-Derived Stem Cells Isolated from Rats during the Course of Diabetes

Lixia Wen [1,2], Peng Liu [3], Qi Chen [3], Jiayuan Ge [3], Bo Jia [4,*] and Qin Li [1,3,*]

1   The First School of Clinical Medicine, Southern Medical University, Guangzhou 510010, China; wenlixia2014@126.com

2   Department of Plastic Surgery, The People's Hospital of China Three Gorges University, Yichang 443000, China

3   Department of Plastic Surgery, General Hospital of Southern Theater Command of PLA, Guangzhou 510010, China; liupengsyd@163.com (P.L.); gzucmchenqi@163.com (Q.C.); Gvivitrip@gmail.com (J.G.)

4   Department of Oral and Maxillofacial Surgery, Stomatological Hospital, Southern Medical University, Guangzhou 510010, China

*   Correspondence: dentist-jia@163.com (B.J.); gzzxwk@163.com (Q.L.)

Abstract: Background: To characterize the impaired of proliferation, apoptosis, and angiogenic activity in ASCs isolated at different stages of the disease course from rats with type 1 diabetes mellitus (T1DM) rats induced by streptozotocin (STZ). Methods: Adipose tissues of the epididymis were harvested at 0, 4, 8, 12, and 16 weeks after the induction of T1DM in rats and from normal rats at the same time points and the morphological variations were detected by Oil red O staining. ASCs were collected from adipose tissues. Cell proliferation, apoptosis, vascular endothelial growth factor (VEGF), and basic fibroblast growth factor (bFGF) expression were assessed. Results: With the prolongation of the disease course, the size and the morphology of adipocytes were distorted, and intracellular lipid droplets became smaller. After 4 weeks, the proliferation of ASCs was decreased, while apoptosis in ASCs was increased. Furthermore, as the disease proceeded, proliferation decreased and apoptosis increased. VEGF and bFGF expression in ASCs from diabetic rats was downregulated at 8 weeks. Conclusion: At 4 weeks after T1DM induction, the proliferation of ASCs decreased and apoptosis increased. The expression of angiogenic factors in ASCs declined at 8 weeks after T1DM induction. The changes in the proliferation, apoptosis, and angiogenic activity are related to the prolongation of disease course.

Keywords: diabetes mellitus type 1; course of disease; rat models; adipose-derived stem cells; impairs

1. Introduction

Type 1 diabetes mellitus (T1DM) is an endocrine disorder characterized by insulin deficiency usually due to autoimmune pancreatic β-cell destruction, and results in hyperglycemia and related complications such as ketoacidosis, cardiovascular disease, nephropathy, and retinopathy [1,2]. T1DM can occur at any age, but commonly presents in childhood or adolescence, often with classic symptoms such as polyuria, polydipsia, polyphagia, and sudden weight loss [2,3]. Type 2 diabetes mellitus (T2DM) is a common endocrine disorder characterized by variable degrees of insulin resistance and deficiency that result in hyperglycemia [1,2]. T2DM is often identified through routine screening beginning in middle age or through the targeted screening of overweight or obese adults of any age with risk factors such as metabolic syndrome, polycystic ovary syndrome, a history of gestational diabetes, or other concerning familial, clinical, or demographic characteristics [1,2]. The number of people worldwide with T1DM and T2DM worldwide is expected to increase to 693 million by 2045 [4].

Foot ulcers are found in about 6.3% of diabetic patients worldwide and seriously affect their quality of life [5–7]. Patients with DM are prone to vascular lesions, which is strongly associated with angiogenic disorder, endogenous regeneration obstruction, decreased levels of growth factors, impaired collagen synthesis, and dysregulation of proteolytic enzymes [8,9]. As a result, diabetic wound healing is often impaired by ischemia [6,7].

Cell therapy has emerged as a hot topic in research into improving chronic wound healing. Adipose-derived stem cells (ASCs) are mesenchymal stem cells derived from adipose tissue, which is abundant in the human body and easily isolated. Previous studies have demonstrated their great potential in clinical applications of stem cell transplantation therapy. Besides, adipose tissue is also involved in systemic inflammation in abnormal metabolic states. DM can induce dysfunctional ASCs, while ASCs can promote angiogenesis and bone regeneration [10]. On the other hand, the angiogenic factors in ASCs decreased in patients with diabetes [11]. Mesenchymal stem cell markers are downregulated in the subcutaneous adipose tissue of DM rats, and DM impairs the efficiency of spontaneous self-repair and autologous stem cell therapy [12]. Gong et al. [13]. confirmed that a simulated DM microenvironment affected the proliferation, apoptosis, homeostasis, endothelial cell migration, and collagen synthesis of ASCs, leading to delayed wound healing.

As the course of DM progresses, various systematic and cellular damages occur and intensify [14,15]. Nevertheless, the effect of DM duration on ASC-related characteristics has not been studied. This study aimed to investigate the changes in proliferation, apoptosis, and expression of pro-angiogenic factors (vascular endothelial growth factor (VEGF) and basic fibroblast growth factor (bFGF)) in ASCs from a T1DM rat model, and whether these changes were related to the prolonged course of the disease. The results should provide a theoretical direction for the optimal use of ASCs to treat stalled DM wounds.

2. Materials and Methods

2.1. T1DM Rat Models and Grouping

The Ethics Committee of the General Hospital of Southern Theater Command (Guangzhou, China), affiliated to Southern Medical University, approved all the animal experiments. In total, 70 SPF male Sprague-Dawley (SD) rats, weighing 180–220 g and about 6–8 weeks old, were purchased from Guangdong Animal Experimental Center (Guangdong, China).

All the rats were fed for 1 week to adapt the environment and then randomly divided into T1DM ($n = 45$) and normal ($n = 25$) groups. The rats in the T1DM group were injected with streptozotocin (STZ) (50 mg/kg) intraperitoneally after fasting for 8 h and rats in the normal group were injected with equivalent amount of sodium citrate buffer. After 72 h, caudal vein blood glucose was measured; the model was considered successful when the blood glucose level was ≥ 16.7 mmol/L and remained stable. After the model was established, blood glucose was monitored weekly, and rats with a blood glucose level of <16.7 mmol/L were excluded from the T1DM group. Diabetes symptoms were observed and weight changes were monitored. All rats were fed with the same diet. The rats were anesthetized with 0.8% pentobarbital sodium overdose at 0, 4, 8, 12, and 16 weeks after T1DM induction (8 rats in each group) or normal rats (5 rats in each group) at the same time points. Bilateral epididymal fat pads were excised from all rats and then divided into two parts under aseptic condition. One part was placed in 4% paraformaldehyde solution for fixation, and the other part was processed immediately for ASC extraction.

2.2. Histological Observation

After fixation with 4% paraformaldehyde, dehydration, and embedding in OCT (4583, Sakura Finetek Europe B.V., Alphen an den Rijn, The Netherlands), the tissue samples were cut into 8–10 μm thick sections using a frozen slicer, and then pasted directly on a slide. The frozen sections were reheated and dried for 10 min. Oil red O working solution (G1016, Wuhan Google Biology Co., Ltd., Wuhan, China) was added and incubated for 10–15 min. The slides were rinsed with 75% alcohol for 2 s and water for 1 min. Harris hematoxylin

was used for counterstaining for 1–2 min. The slides were rinsed with running water, 1% hydrochloric acid alcohol for several seconds, running water, ammonia, and running water again. The sections were sealed with glycerin gelatin. The slides were observed under an inverted fluorescence microscope and photographed. The lipid droplets are shown as orange-red or bright red; the nuclei are blue.

2.3. ASC Extraction

The fresh epididymal fat pads were cut up and digested with type I collagenase (BSO32A, Sigma, St Louis, MO, USA) for 1 h in a 37 °C water bath. The cells were filtered using a 40 μm cell sieve and centrifuged (1000 r/min, 5 min). The cells were rinsed with 3 mL of sodium citrate buffer and centrifuged (1000 r/min, 5 min), twice. Complete medium (45 mL of low-sugar DMEM, 5 mL FBS of fetal bovine serum, and 1 mL of penicillin/streptomycin) was used to resuspend and culture the cells in an incubator at 37 °C with 5% CO_2. The medium was changed every 24 h. When a confluence of 80–90% was reached, the cells were digested and subcultured. The cells from the second passage (Passage 2) were used for the experiments.

2.4. Flow Cytometry

The stem cell surface markers in three samples from each group were detected by flow cytometry. The ASCs were cultivated to Passage 3 and grown to 80–90% confluence; then, the cells were digested and the cell suspension was collected into a sterile centrifuge tube. After centrifugation and resuspension, the cell density was adjusted to 10^6 cells/mL in PBS. The suspension was separated into six equal parts: blank control group (FITC), blank control group (PE), CD45-FITC antibody (554877, Pharmingen, BD Biosciences, Franklin Lake, NJ, USA), CD44-FITC antibody (NBP1-41266F, Novus Biologicals, Littleton, CO, USA), CD90-FITC antibody (554897, Pharmingen, BD Biosciences, Franklin Lake, NJ, USA), and CD34-PE antibody (NB600-1071PE, Novus Biologicals, Littleton, CO, USA). The two blank control groups were required for voltage gating in flow cytometry detection. The samples of each group were mixed and incubated at 4 °C in the dark for 40 min. The supernatant was centrifuged and discarded, and the pellet was resuspended in PBS. The cells were centrifuged, the supernatant was discarded, resuspended in PBS, centrifuged again, the supernatant was discarded, and finally the pellet was resuspended in 500 μL of PBS. The samples were filtered using a 40 μm cell sieve, and the CD molecules on the surface of the ASCs were detected using a FACSCalibur system (BD Biosciences, Franklin Lake, NJ, USA).

2.5. Cell Proliferation

Five samples at Passage 2 were collected, digested in a single-cell suspension, and inoculated in 96-well plates at a density of 2000 cells/well in complete medium. Each sample was tested in five replicates. Five plates were set up for each time point. Each plate was set with three blank wells (no cells, equal amount of complete medium). The margin wells were filled with sterile PBS. OD450 was read in microplate reader on days 1, 3, 5, 7, and 9 by CCK-8 (Dojindo Molecular Technologies, Kimamoto, Japan). The medium was changed every 2 days before the cell count. The growth curves were plotted.

2.6. TUNEL Staining

Passage 3 ASCs were prepared at 1×10^4 cells/mL, fixed with 4% paraformaldehyde, and stained with TUNEL (Sigma, St. Louis, MO, USA) in accordance with the manufacturer's instructions. The slides were counterstained with DAPI at room temperature in the dark for 10 min and then washed with PBS (pH 7.4) three times, each for 5 min. The sections were observed under a fluorescence microscope, and the images were collected. The number of apoptotic cells in three random fields was detected using a fluorescence microscope.

2.7. Immunofluorescence for VEGF and bFGF

Passage 3 ASCs were digested, resuspended, and then cultured at 10^4 cells/well in 6-well culture plates overnight at 37 °C in an incubator with 5% CO_2. The cells were fixed with 4% paraformaldehyde for 20 min and washed with PBS three times, each for 5 min. After the slides were lightly dried, a chemical pen (GT1001, Genentech, Inc., San Francisco, CA, USA) was used to draw a circle in the middle of the cover glass where the cells were evenly distributed, and BSA was added to the circle and incubated for 30 min. Primary anti-VEGF (GB1, 1:100, Servicebio, Woburn, MA, USA) and bFGF (SC-271847, 1:100, Santa Cruz Biotechnology, Santa Cruz, CA, USA) were added and incubated in a wet box at 4 °C overnight. The secondary anti-CY3 goat anti-mouse (GB21301, Servicebio, Woburn, MA, USA) and 488 goat anti-rabbit (GB25303, Servicebio, Woburn, MA, USA) were added and incubated in the dark for 50 min at room temperature. The slides were washed with PBS (pH 7.4) three times, each for 5 min. The slides were counterstained with DAPI at room temperature in the dark for 10 min, and washed with PBS (pH 7.4) three times, each for 5 min. The slides were observed and images were collected using a microscope (Nikon, Tokyo, Japan). Positive expression was indicated by luciferin-labeled red light (bFGF) and green light (VEGF). ImageJ was used to quantify the percentage of positive cells.

2.8. Real-Time Quantitative PCR

An RNA extraction kit (LS1040, Promega, Shanghai, China) was used to extract the total RNA from Passage 3 ASCs from each group. cDNA was obtained using a reverse transcription kit (K1622, Thermo Fisher Scientific, Waltham, MA, USA), and then real-time fluorescence quantitative PCR was performed. The reaction system of 20 µL contained 4 µL of cDNA, 0.6 µL of each primer, 10 µL of SYBR Green Master Mix, and 4.8 µL of ddH_2O. Table 1 presents the primer sequences. The PCR amplification sequence was performed as follows: pre-denaturation at 95 °C for 10 min, denaturation at 95 °C for 15 s, and annealing at 60 °C for 30 s, for a total of 40 cycles, with a final extension at 72 °C for 45 s. The expression level of each target gene was standardized using GAPDH of the same sample as the internal reference gene. The relative expression level of each gene was calculated using the $2^{-\Delta\Delta ct}$ method.

Table 1. Primers used for qPCR.

Genes	Sequences (5′–3′)
R-VEGF-S	AATGATGAAGCCCTGGAGTGC
R-VEGF-A	TAAACCGGGATTTCTTGCGC
R-b-FGF-S	CCTGGCTATGAAGGAAGATGGAC
R-b-FGF-A	CCAGTTCGTTTCAGTGCCACAT
R-GAPDF-S	TTCCTACCCCCAATGTATCCG
R-GAPDF-A	CATGAGGTCCACCACCCTGTT

2.9. Statistical Analysis

All statistical analysis was performed using SPSS 17.0 (IBM, Armonk, NY, USA), and a *p* value of < 0.05 was considered significant. The data are presented as mean ± SEM and analyzed using ANOVA, and the Bonferroni test was used for pairwise comparison (α level was set at 0.008).

3. Results

3.1. Model Success

The rats in each group were generally in good health before modeling, with no significant differences in blood glucose or weight. By 3 days after modeling, the rats in the T1DM group began to manifest polydipsia, polyphagia, polyuria, and hypoactivity, with high levels of random blood glucose ($\geq$16.7 mmol/L) and a body weight obviously lower than the control (Figure 1). In the advanced stage (8 weeks after modeling), the diabetic rats exhibited hypoactivity, listlessness, lusterless hair, and even cataracts.
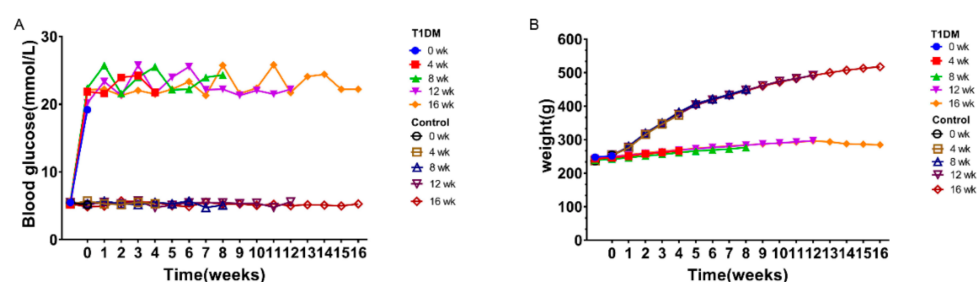
Figure 1. Weekly blood glucose and weight measurements of the SD rats. (**A**) Weekly measurements showing that the blood glucose level of all rats in the T1DM group was ≥16.7 mmol/L, which was obviously higher than the control group. (**B**) Weekly weight measurement showing that weight of all rats in the T1DM group was not significantly changed, but increased gradually in the control group.

3.2. Histological Observation of Adipose Tissue

Oil red O staining showed that fat droplets in adipose cells were colored orange or red, while the nucleus was stained blue. In the control group, the morphology and quantity of fat cells did not change with time. However, in the T1DM group, as the disease progressed, the lipid droplets in fat cells shrunk, the cell volume decreased, and morphological abnormalities were observed (Figure 2).
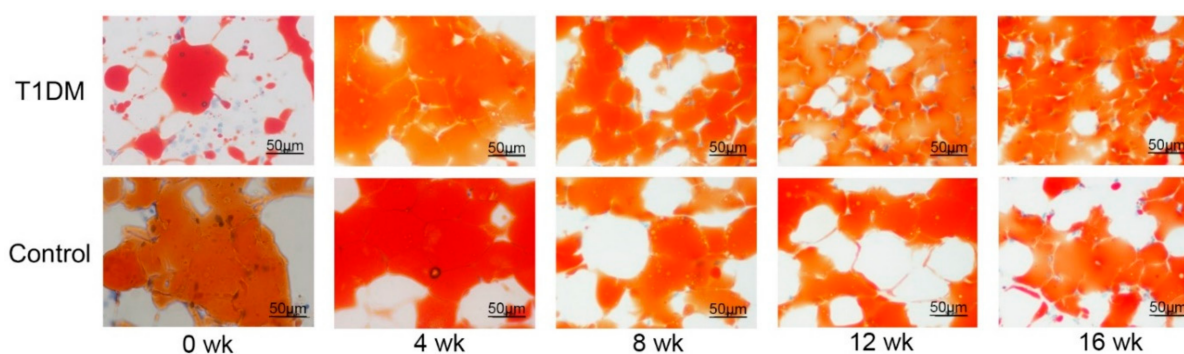

Figure 2. Histological observation of adipose tissues. Epididymal adipose tissues were collected at 0, 4, 8, 12, and 16 weeks after T1DM induction or from normal control rats at the same time points and stained with Oil red O. Magnification = 400×.

3.3. Morphology of the ASCs

ASCs were successfully isolated from epididymal adipose tissue. Adherent cells were seen at 8 h after the primary inoculation, and the morphology of the ASCs varied after 48 h. Most cells gradually developed into a spindle shape; the culture plate reached 80–90% confluence in 9–10 days. Cell growth significantly accelerated after passage, and passage could be repeated in 4–5 days. Passage 3 cells from the T1DM and control groups were identical in shape, with long spindles, arranged like fish, with no obvious differences in morphology (Figure 3).

3.4. Flow Cytometric Detection of CD Molecules on the Surface of ASCs

Flow cytometric detection showed positive expression of CD44 and CD90 in Passage 3 ASCs from each group, and negative expressions of CD34 and CD45, confirming that the cultured cells were mesenchymal stem cells. There were few differences between the T1DM and control groups.

3.5. ASC Proliferation

The value of OD450 is positively correlated with the amount of living cells. As Figure 4 shows, the growth of ASCs in the T1DM and control groups exhibited an inverted S-shape curve. The ASCs in each group were in the logarithmic growth stage from day 3 to day 7,

with a maximum growth rate on day 5, and entered the plateau stage on day 7. The growth curve decreased on day 7, suggesting the possibility of cell death.
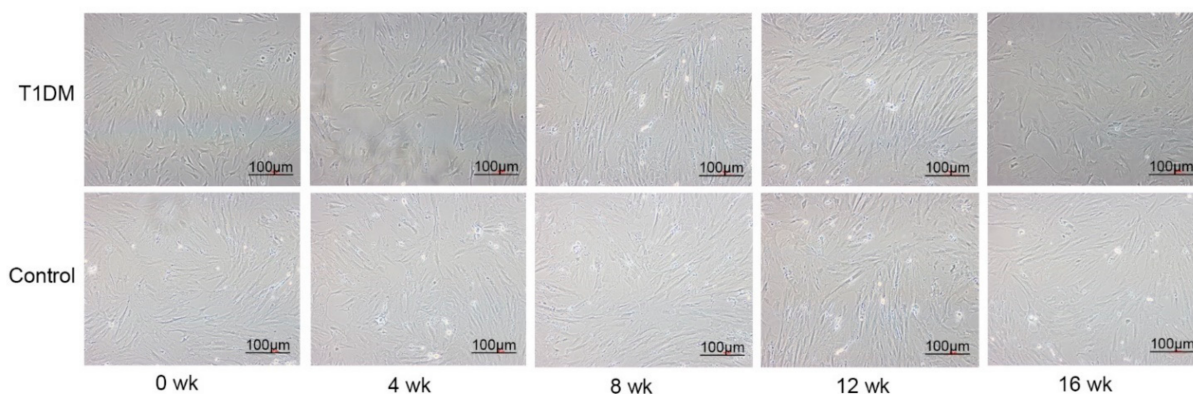

Figure 3. ASC morphology. ASCs collected at 0, 4, 8, 12, and 16 weeks after T1DM induction and from control rats at the same time points exhibited similar morphology. Magnification = $100\times$.
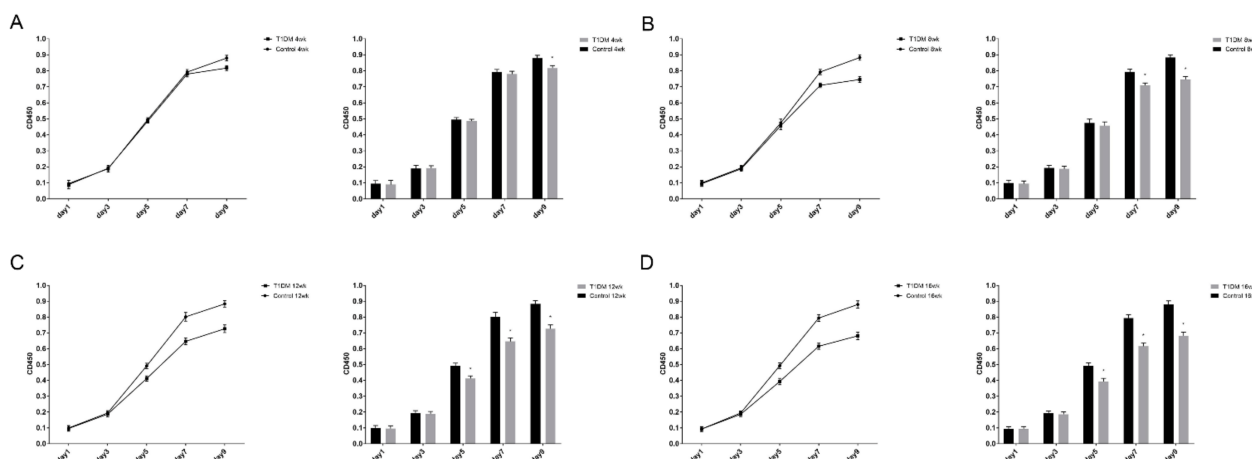

Figure 4. ASC proliferation. (**A**): At 4 weeks, proliferation decreased at day 9 compared with control groups of the same time point. *, $p < 0.05$. (**B**): At 8 weeks T1DM groups, proliferation diminished at day 7, day 9, compared with control groups. *, $p < 0.05$. (**C,D**): At 12 or 16 weeks T1DM groups, proliferation lowered at day 5, day 7, day 9, compared with control groups. *, $p < 0.05$.

There were no differences in proliferations at 0 weeks between the T1DM and control groups. After 4 weeks, in the T1DM group, proliferation capacity was decreased at day 9 compared with the control group at the same time point (Figure 4A). After 8 weeks, in the T1DM group, the proliferation capacity diminished, respectively, at day 7 and day 9 (Figure 4B), compared with control group at the same time point. After 12 or 16 weeks, in the T1DM group, proliferation was reduced at day 5, day 7, and day 9 (Figure 4C,D) compared with the control group at the same time point.

3.6. Effect of T1DM Course on Apoptosis in Passage 3 ASCs

There were no statistically significant differences in apoptosis of Passage 3 ASCs between the control group. There were no differences between the 0 week T1DM group and the control group. Apoptosis increased at 4, 8, 12, or 16 weeks after T1DM induction compared with control group at the same time point. The intra-group comparison in the T1DM group showed that apoptosis rate in ASCs increased with the course of diabetes (Figure 5).
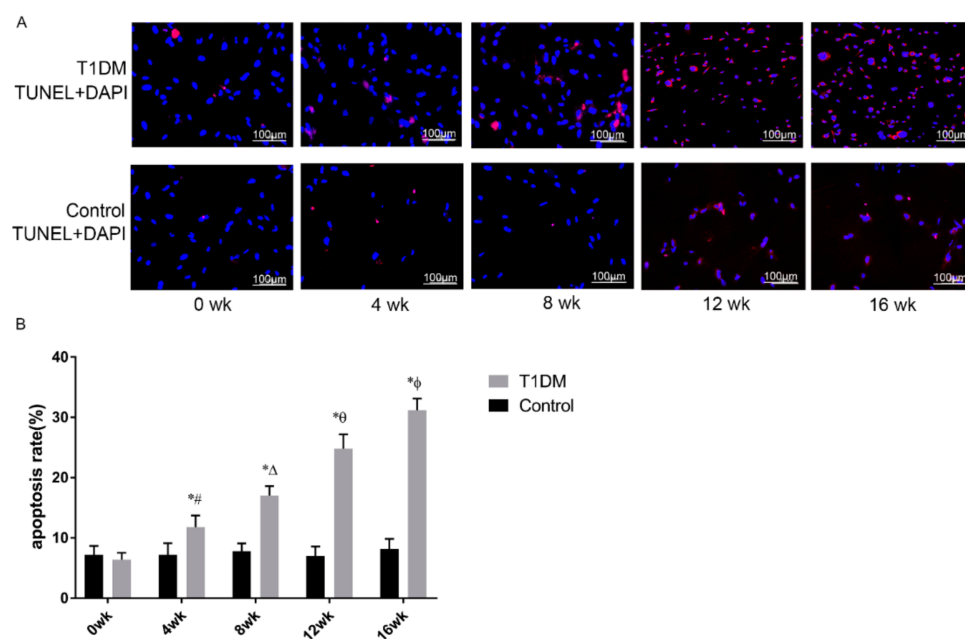
Figure 5. ASC apoptosis. (**A**): Apoptosis in Passage 3 ASCs in the T1DM group after 0, 4, 8, 12, and 16 weeks or control group at the same time points was detected with TUNEL staining. Scale 200×. (**B**): Apoptosis rate was higher at 4, 8, 12, and 16 weeks in T1DM group compared with control group at the same time point. *, $p < 0.05$. Intra-group comparison in the T1DM group showed that the apoptosis rate of ASCs gradually increased with the prolongation of the course of diabetes. #, $p < 0.05$, vs. 0 week of T1DM. Δ, $p < 0.05$, vs. 4 weeks of T1DM. θ, $p < 0.05$, vs. 8 weeks of T1DM. Φ, $p < 0.05$, vs. 12 weeks of T1DM.

3.7. Expression of VEGF and bFGF in ASCs

Immunofluorescence showed that the protein expression of VEGF and bFGF in ASCs was concentrated in the cytoplasm, and that they were co-located in ASCs (Figure 6A). There was no significant differences in VEGF and bFGF protein expression among the control group. The protein expression of VEGF or FGF was downregulated at 8, 12, and 16 weeks in the T1DM group compared with control group at the same time point. Furthermore, this downregulation escalated with the course of diabetes (Figure 6B,C).

Additionally, qPCR results showed that there were no statistically significant differences in VEGF and bFGF mRNA expression among the control group. The mRNA expression of VEGF and bFGF was downregulated at 8, 12, and 16 weeks in the T1DM group compared with the control group at the same time point. The mRNA expression of VEGF and bFGF continued to decrease with the prolongation of the course of diabetes ($p < 0.05$) (Figure 7).
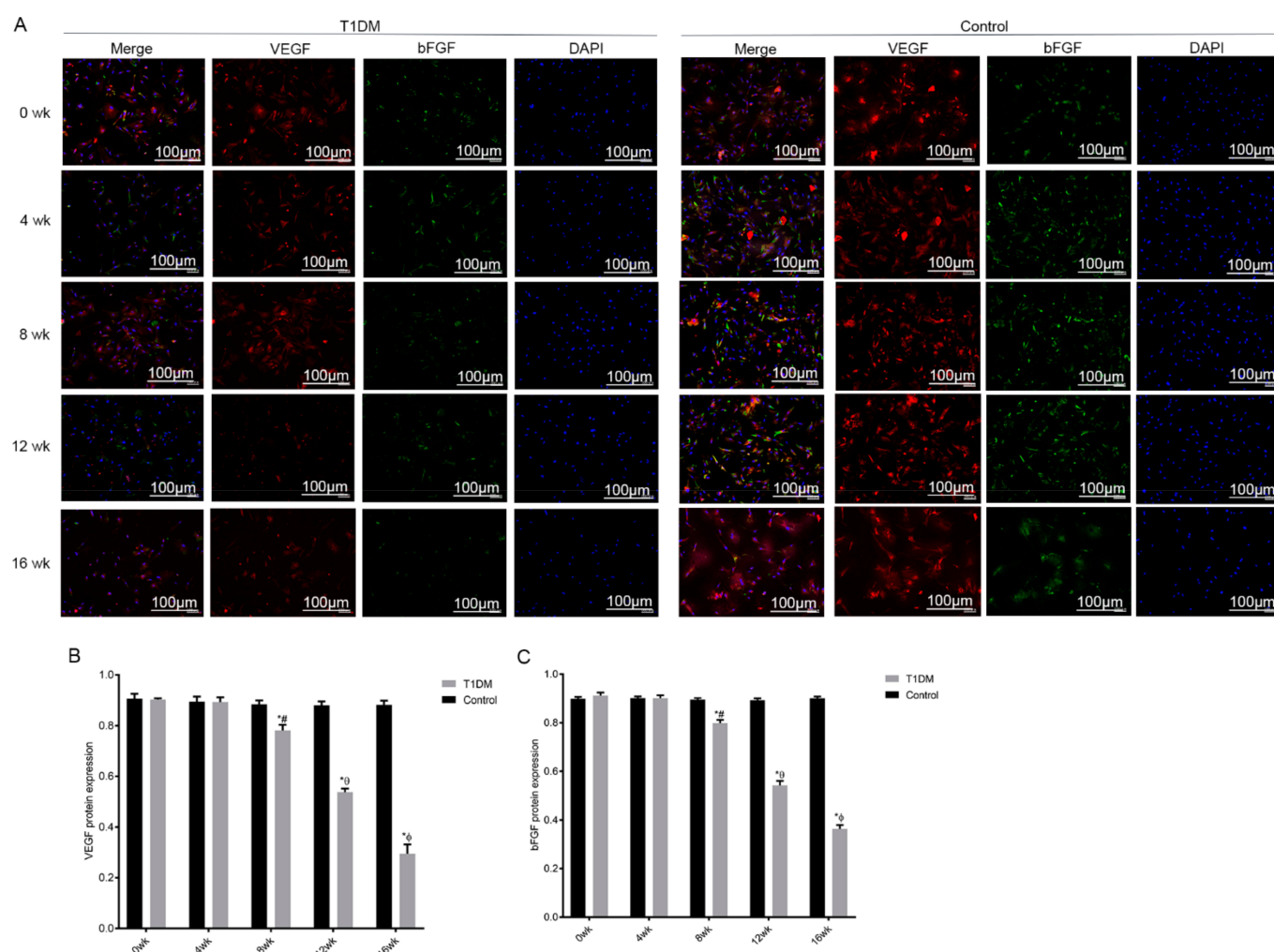
Figure 6. The protein expression and co-localization of VEGF and bFGF in ADSCs. (**A**): Immunofluorescence showed that the protein expression of VEGF and bFGF in ASCs was mainly concentrated in the cytoplasm, and that they were co-located in ASCs. Magnification = 200×. (**B**,**C**): The protein expression of VEGF and bFGF was downregulated at 8, 12, and 16 weeks in the T1DM group compared with the control group at the same time point. *, $p < 0.05$. The expression of VEGF and bFGF continued to downregulate with the prolongation of the course of diabetes. #, $p < 0.05$, vs. 4 weeks of T1DM. θ, $p < 0.05$, vs. 8 weeks of T1DM. Φ, $p < 0.05$, vs. 12 weeks of T1DM.
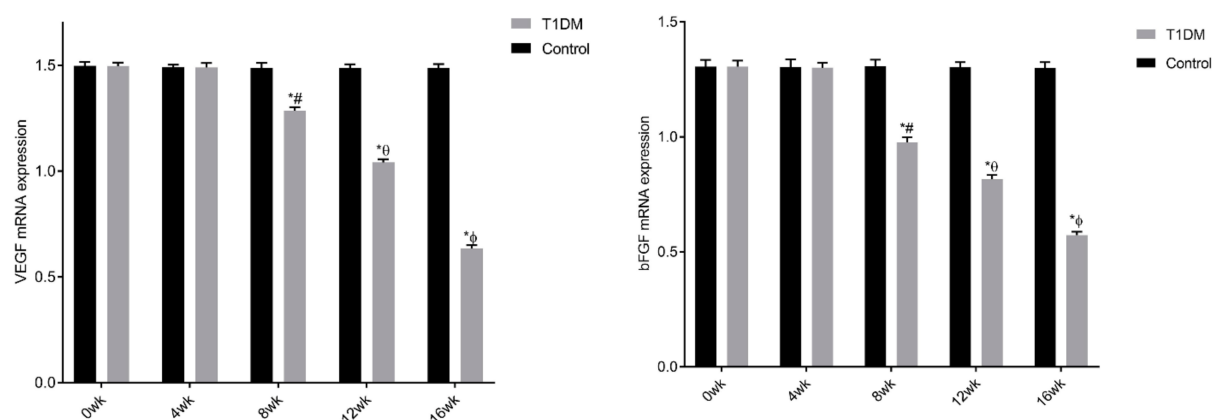

Figure 7. The mRNA expression of VEGF and bFGF in ADSCs. The mRNA expression of VEGF and bFGF was downregulated at 8, 12, and 16 weeks in T1DM group compared with control group at the same time point. *, $p < 0.05$. The mRNA expression of VEGF and bFGF continued to downregulate with the prolongation of the course of diabetes. #, $p < 0.05$, vs. 4 weeks of T1DM. θ, $p < 0.05$, vs. 8 weeks of T1DM. Φ, $p < 0.05$, vs. 12 weeks of T1DM.

4. Discussion

The function of ASCs may be impaired gradually over the course of DM. Therefore, this study aimed to investigate the effects of the course of T1DM on proliferation, apoptosis, and VEGF and bFGF expression in ASCs. The results indicated that the adipose tissue from the T1DM rat model changed with the prolongation of the disease course. The proliferation of ASCs was decreased while apoptosis was increased after 4 weeks of T1DM. The expression of pro-angiogenic factors was downregulated after 8 weeks of T1DM and was exacerbated with the disease course.

Adipose tissue is a typical energy storage tissue [16]. The current evolutionary and developmental studies compellingly suggest that adipose tissue is deeply involved in systemic inflammation in DM [16–19]. DM seriously affects lipid metabolism [20], and oxidative stress induced by DM is a major reason for impaired endothelial function and regeneration [21–23]. Dysfunctional vascular endothelial cells and decreased vascular elasticity are causative of the reduction of effective blood perfusion in diabetic wounds [21–23]. When the body suffers injury stress, local neovascularization will deliver nutrients, bioactive proteins, and oxygen to the tissues surrounding the wound. Simultaneously, ischemia exerts a negative role in wound repair. Angiogenesis is prompted by a variety of cytokines, including bFGF, angiogenic factor-1 (Ang-1), and, most importantly, VEGF. Serum VEGF concentrations are elevated in children and adolescents with DM [24]. Blood glucose control affects serum VEGF level, and microvascular complications are correlated with augmented serum VEGF in patients with DM [24]. VEGF is currently recognized as the growth factor most related to angiogenesis [25]. VEGF is a dimer glycoprotein with uniform gene coding, which directly stimulates the movement, proliferation, and differentiation of vascular endothelial cells, as well as the permeability of microvessels [25]. In early stages of tissue injuries, VEGF increases vascular permeability, stimulating vascular endothelial cell proliferation, differentiation, and proliferation, establish collateral circulation, mediates cell signal transduction pathway, participates in vascular smooth muscle relaxation, and increases tissue oxygen supply, thereby reducing local hypoxia injury [26]. The baseline serum VEGF levels are low but increased by ischemia and hypoxia; therefore, local VEGF will be significantly increased, stimulating the endothelial progenitor cells, promoting angiogenesis, and improving microcirculation. After the occurrence of transient ischemia, VEGF will have an effect on the VEGF receptor on the surface of the cell membrane in the diseased tissue, achieving anti-apoptosis, pro-angiogenesis, and anti-inflammatory effects [26]. However, Lijnen et al. [27] found that blocking VEGF-B signaling enables PLGF to activate VEGFR1 signaling and promote vascularization in adipose tissue, which then increases glucose tolerance.

Several studies have been carried out to prove the efficacy of ASCs, biomaterials, and growth factors in regenerative and plastic surgeries. However, complete knowledge of the mechanisms of interactions among ASCs, growth factors, and biomaterials will go a long way to supporting the success of plastic surgeries [28].

ASCs are a group of cells abounding in fat, with the ability to migrate to damaged sites and boost tissue repair by promoting angiogenesis [29]. ASCs can not only proliferate and differentiate into different types of tissue cells, but also stimulate and accelerate tissue angiogenesis by secreting VEGF, bFGF, and other cytokines, which then facilitates local capillaries and collateral circulation, and improve blood supply in the affected limbs, which is meaningful for skin wounds in patients with DM [30–33]. ASCs undergo phenotypic changes in abnormal metabolic states, leading to impaired cell differentiation [34]. Diabetic ASCs exhibit lower neovascularization potential in vitro [35]. Studies have shown that diabetic ASCs manifest dysfunctions related to proliferation, apoptosis, and angiogenesis, resulting in the obstructed repair of diabetic wounds [34,36,37].

5. Conclusions

In conclusion, this study showed that adipose tissue from T1DM model rats exhibits multiple changes with the course of T1DM. At 4 weeks after T1DM induction, the prolif-

eration of ASCs decreased, while apoptosis increased. The expression of pro-angiogenic factors was downregulated at 8 weeks of T1DM and exacerbated by the disease course.

Of course, as this is an in vivo and in vitro study, the results will have to be validated in humans. Nevertheless, the results will be of use for the design of more optimal cell-based therapeutic strategies for stalled wounds in patients with DM.

References

1. American Diabetes Association. Introduction: Standards of medical care in diabetes—2020. *Diabetes Care* **2020**, *43*, S1–S2. [CrossRef] [PubMed]
2. American Diabetes Association. Diagnosis and classification of diabetes mellitus. *Diabetes Care* **2014**, *37* (Suppl. 1), S81–S90. [CrossRef]
3. Daneman, D. Type 1 diabetes. *Lancet* **2006**, *367*, 847–858. [CrossRef]
4. Cho, N.H.; Shaw, J.E.; Karuranga, S.; Huang, Y.; da Rocha Fernandes, J.D.; Ohlrogge, A.W.; Malanda, B. Idf diabetes atlas: Global estimates of diabetes prevalence for 2017 and projections for 2045. *Diabetes Res. Clin. Pract.* **2018**, *138*, 271–281. [CrossRef] [PubMed]
5. Zhang, P.; Lu, J.; Jing, Y.; Tang, S.; Zhu, D.; Bi, Y. Global epidemiology of diabetic foot ulceration: A systematic review and meta-analysis (dagger). *Ann. Med.* **2017**, *49*, 106–116. [CrossRef] [PubMed]
6. Van Hattem, S.; Bootsma, A.H.; Thio, H.B. Skin manifestations of diabetes. *Clevel. Clin. J. Med.* **2008**, *75*, 772–774. [CrossRef] [PubMed]
7. Chatterjee, S.; Khunti, K.; Davies, M.J. Type 2 diabetes. *Lancet* **2017**, *389*, 2239–2251. [CrossRef]
8. Boulton, A.J.; Vileikyte, L.; Ragnarson-Tennvall, G.; Apelqvist, J. The global burden of diabetic foot disease. *Lancet* **2005**, *366*, 1719–1724. [CrossRef]
9. Lee, K.B.; Choi, J.; Cho, S.B.; Chung, J.Y.; Moon, E.S.; Kim, N.S.; Han, H.J. Topical embryonic stem cells enhance wound healing in diabetic rats. *J. Orthop. Res.* **2011**, *29*, 1554–1562. [CrossRef] [PubMed]
10. Nawrocka, D.; Kornicka, K.; Szydlarska, J.; Marycz, K. Basic fibroblast growth factor inhibits apoptosis and promotes proliferation of adipose-derived mesenchymal stromal cells isolated from patients with type 2 diabetes by reducing cellular oxidative stress. *Oxid. Med. Cell. Longev.* **2017**, *2017*, 3027109. [PubMed]
11. Wallner, C.; Abraham, S.; Wagner, J.M.; Harati, K.; Ismer, B.; Kessler, L.; Zollner, H.; Lehnhardt, M.; Behr, B. Local application of isogenic adipose-derived stem cells restores bone healing capacity in a type 2 diabetes model. *Stem Cells Transl. Med.* **2016**, *5*, 836–844. [CrossRef] [PubMed]
12. Ferrer-Lorente, R.; Bejar, M.T.; Tous, M.; Vilahur, G.; Badimon, L. Systems biology approach to identify alterations in the stem cell reservoir of subcutaneous adipose tissue in a rat model of diabetes: Effects on differentiation potential and function. *Diabetologia* **2014**, *57*, 246–256. [CrossRef] [PubMed]
13. Gong, J.H.; Dong, J.Y.; Xie, T.; Lu, S.L. The influence of ages environment on proliferation, apoptosis, homeostasis, and endothelial cell differentiation of human adipose stem cells. *Int. J. Low. Extrem. Wounds* **2017**, *16*, 94–103. [CrossRef] [PubMed]
14. Jang, M.; Kim, H.; Lea, S.; Oh, S.; Kim, J.S.; Oh, B. Effect of duration of diabetes on bone mineral density: A population study on east asian males. *BMC Endocr. Disord.* **2018**, *18*, 61. [CrossRef] [PubMed]

15. Voigt, M.; Schmidt, S.; Lehmann, T.; Kohler, B.; Kloos, C.; Voigt, U.A.; Meller, D.; Wolf, G.; Muller, U.A.; Muller, N. Correction: Prevalence and progression rate of diabetic retinopathy in type 2 diabetes patients in correlation with the duration of diabetes. *Exp. Clin. Endocrinol. Diabetes* **2018**, *126*, e2. [CrossRef]

16. Lenz, M.; Arts, I.C.W.; Peeters, R.L.M.; de Kok, T.M.; Ertaylan, G. Adipose tissue in health and disease through the lens of its building blocks. *Sci. Rep.* **2020**, *10*, 10433. [CrossRef]

17. Zatterale, F.; Longo, M.; Naderi, J.; Raciti, G.A.; Desiderio, A.; Miele, C.; Beguinot, F. Chronic adipose tissue inflammation linking obesity to insulin resistance and type 2 diabetes. *Front. Physiol.* **2019**, *10*, 1607. [CrossRef]

18. Henriques, F.; Bedard, A.H.; Batista, M.L.J. Adipose tissue inflammation and metabolic disorders. In *Adipose Tissue Update*; Szablewski, L., Ed.; IntechOpen: London, UK, 2019.

19. Carrillo, J.L.M.; Campo, J.O.M.D.; Coronado, O.G.; Gutierrez, P.T.V.; Cordero, J.F.C.; Juarez, J.V. Adipose tissue and inflammation. In *Adipose Tissue*; Szablewski, L., Ed.; IntechOpen: London, UK, 2018.

20. Athyros, V.G.; Doumas, M.; Imprialos, K.P.; Stavropoulos, K.; Georgianou, E.; Katsimardou, A.; Karagiannis, A. Diabetes and lipid metabolism. *Hormones* **2018**, *17*, 61–67. [CrossRef]

21. Yu, C.G.; Zhang, N.; Yuan, S.S.; Ma, Y.; Yang, L.Y.; Feng, Y.M.; Zhao, D. Endothelial progenitor cells in diabetic microvascular complications: Friends or foes? *Stem Cells Int.* **2016**, *2016*, 1803989. [CrossRef]

22. Shi, Y.; Vanhoutte, P.M. Macro- and microvascular endothelial dysfunction in diabetes. *J. Diabetes* **2017**, *9*, 434–449. [CrossRef] [PubMed]

23. Schramm, J.C.; Dinh, T.; Veves, A. Microvascular changes in the diabetic foot. *Int. J. Low. Extrem. Wounds* **2006**, *5*, 149–159. [CrossRef]

24. Chiarelli, F.; Spagnoli, A.; Basciani, F.; Tumini, S.; Mezzetti, A.; Cipollone, F.; Cuccurullo, F.; Morgese, G.; Verrotti, A. Vascular endothelial growth factor (vegf) in children, adolescents and young adults with type 1 diabetes mellitus: Relation to glycaemic control and microvascular complications. *Diabet. Med.* **2000**, *17*, 650–656. [CrossRef] [PubMed]

25. Eelen, G.; Treps, L.; Li, X.; Carmeliet, P. Basic and therapeutic aspects of angiogenesis updated. *Circ. Res.* **2020**, *127*, 310–329. [CrossRef]

26. Johnson, K.E.; Wilgus, T.A. Vascular endothelial growth factor and angiogenesis in the regulation of cutaneous wound repair. *Adv. Wound Care* **2014**, *3*, 647–661. [CrossRef]

27. Lijnen, H.R.; Christiaens, V.; Scroyen, I.; Voros, G.; Tjwa, M.; Carmeliet, P.; Collen, D. Impaired adipose tissue development in mice with inactivation of placental growth factor function. *Diabetes* **2006**, *55*, 2698–2704. [CrossRef]

28. Zarei, F.; Negahdari, B. Recent progresses in plastic surgery using adipose-derived stem cells, biomaterials and growth factors. *J. Microencapsul.* **2017**, *34*, 699–706. [CrossRef] [PubMed]

29. Zhao, L.; Johnson, T.; Liu, D. Therapeutic angiogenesis of adipose-derived stem cells for ischemic diseases. *Stem Cell Res. Ther.* **2017**, *8*, 125. [CrossRef] [PubMed]

30. Charles-de-Sa, L.; Gontijo-de-Amorim, N.F.; Takiya, C.M.; Borojevic, R.; Benati, D.; Bernardi, P.; Sbarbati, A.; Rigotti, G. Antiaging treatment of the facial skin by fat graft and adipose-derived stem cells. *Plast. Reconstr. Surg.* **2015**, *135*, 999–1009. [CrossRef] [PubMed]

31. Gruber, H.E.; Somayaji, S.; Riley, F.; Hoelscher, G.L.; Norton, H.J.; Ingram, J.; Hanley, E.N., Jr. Human adipose-derived mesenchymal stem cells: Serial passaging, doubling time and cell senescence. *Biotech. Histochem.* **2012**, *87*, 303–311. [CrossRef] [PubMed]

32. Tollervey, J.R.; Lunyak, V.V. Adult stem cells: Simply a tool for regenerative medicine or an additional piece in the puzzle of human aging? *Cell Cycle* **2011**, *10*, 4173–4176. [CrossRef] [PubMed]

33. Tabit, C.J.; Slack, G.C.; Fan, K.; Wan, D.C.; Bradley, J.P. Fat grafting versus adipose-derived stem cell therapy: Distinguishing indications, techniques, and outcomes. *Aesthetic Plast. Surg.* **2012**, *36*, 704–713. [CrossRef] [PubMed]

34. Rennert, R.C.; Sorkin, M.; Januszyk, M.; Duscher, D.; Kosaraju, R.; Chung, M.T.; Lennon, J.; Radiya-Dixit, A.; Raghvendra, S.; Maan, Z.N.; et al. Diabetes impairs the angiogenic potential of adipose-derived stem cells by selectively depleting cellular subpopulations. *Stem Cell Res. Ther.* **2014**, *5*, 79. [CrossRef] [PubMed]

35. Dzhoyashvili, N.A.; Efimenko, A.Y.; Kochegura, T.N.; Kalinina, N.I.; Koptelova, N.V.; Sukhareva, O.Y.; Shestakova, M.V.; Akchurin, R.S.; Tkachuk, V.A.; Parfyonova, Y.V. Disturbed angiogenic activity of adipose-derived stromal cells obtained from patients with coronary artery disease and diabetes mellitus type 2. *J. Transl. Med.* **2014**, *12*, 337. [CrossRef] [PubMed]

36. Liu, M.H.; Li, Y.; Han, L.; Zhang, Y.Y.; Wang, D.; Wang, Z.H.; Zhou, H.M.; Song, M.; Li, Y.H.; Tang, M.X.; et al. Adipose-derived stem cells were impaired in restricting cd4(+)t cell proliferation and polarization in type 2 diabetic apoe(-/-) mouse. *Mol. Immunol.* **2017**, *87*, 152–160. [CrossRef] [PubMed]

37. Cramer, C.; Freisinger, E.; Jones, R.K.; Slakey, U.P.; Dupin, C.L.; Newsome, E.R.; Alt, E.U.; Izadpanah, R. Persistent high glucose concentrations alter the regenerative potential of mesenchymal stem cells. *Stem Cells Dev.* **2010**, *19*, 1875–1884. [CrossRef] [PubMed]